

normal to the faces of that form. If the assumption of an ellipsoidal particle is well-founded, the breadth should vary in the way suggested by (10b). If not, the departures from the ellipsoidal shape can be examined in the light of Table II of the preceding paper⁷ and an indication of the actual particle shape can be obtained.

The work reported in this and the preceding paper was commenced at the Massachusetts Institute of Technology. It is a pleasure for the writer at this time to express his thanks to Professor J. C. Slater for the privilege of working in his laboratory, and to Professor B. E. Warren for many valuable discussions.

NOVEMBER 15, 1939

PHYSICAL REVIEW

VOLUME 56

The Far Infra-Red Absorption Spectrum and the Rotational Structure of the Heavy Water Vapor Molecule

NELSON FUSON,* H. M. RANDALL, AND D. M. DENNISON
University of Michigan, Ann Arbor, Michigan

(Received September 7, 1939)

An investigation has been made of the spectrum of heavy water vapor (D_2O) in the region from 23μ to 135μ . The instrument used was a self-recording spectrograph of large aperture, using echelette gratings, vacuum thermopile, and a system of filters, shutters, and *reststrahlen* plates to remove higher order spectral impurity. The radiation path in the spectrograph could be evacuated. From this research the experimental positions and relative intensities of 210 pure rotation absorption frequencies were obtained. Absorption maxima were located with an accuracy of about 0.05 cm^{-1} . Lines 0.5 cm^{-1} apart were partially resolved, higher resolution and dispersion being of little advantage since the true width of these absorption lines was of this same order of magnitude. The energy levels of a zeroth-

order approximation to the D_2O asymmetric rotator molecule were computed through quantum number $j=11$, and corrected for zero point vibration and centrifugal stretching in the ground state. A comparison of the positions and intensities of the experimental data with those of the transitions between these "key" levels showed a rather good agreement. These levels were therefore corrected to fit the data, and checked for consistency by means of series regularities and combination relations. In all, 111 distinct energy levels based on the experimental data were computed. A graph of the experimental data contrasted with a similar graph of the transitions based on these corrected levels gives a clear picture of the success of the analysis.

I. INTRODUCTION

A LARGE amount of work has been done on the spectral analysis of ordinary water in its vapor state. Information concerning the molecule as a whole is largely limited to studies of the absorption frequencies occurring in the infra-red region of the electromagnetic spectrum. The vibration-rotation bands of H_2O have been examined a number of times.¹ Since the discovery² of the heavy hydrogen isotope, H^2 (often called deuterium, D), similar studies³ have been made

upon D_2O . In more recent years the extension of the spectrum of H_2O into the region of pure rotation frequencies has been made.⁴ One of these latter studies⁵ succeeded in establishing the rotational energy levels of the ground state with high accuracy. The present investigation was undertaken in the attempt to parallel this H_2O analysis with a similar study of D_2O .

The problem has been to map the far infra-red pure rotation absorption spectrum of heavy

* Now at Rutgers University.

¹ W. W. Sletor, *Astrophys. J.* **48**, 125 (1918); W. W. Sletor and E. R. Phelps, *Astrophys. J.* **62**, 28 (1925); R. Mecke, *Zeits. f. Physik* **81**, 313, 445, 456 (1933); L. G. Bonner, *Phys. Rev.* **46**, 458 (1935); E. Ganz, *Ann. d. Physik* **28**, 445 (1937).

² Urey, Brickwedde and Murphy, *Phys. Rev.* **40**, 1 (1932).

³ J. W. Ellis and B. W. Sorge, *J. Chem. Phys.* **2**, 559 (1934); T. Shidei, *Phys. and Math. Soc. of Japan Proc.* **16**,

362 (1934); E. Bartholome and K. Clusius, *Zeits. f. Elec. Chem.* **40**, 529 (1934); E. F. Barker and W. W. Sletor, *J. Chem. Phys.* **3**, 660 (1935); L. Kellner, *Proc. Roy. Soc.* **159**, a410 (1937).

⁴ H. Rubens, *Berliner Ber. S.* **8** (1931); H. Witt, *Zeits. f. Physik* **28**, 245 (1924); M. Czerny, *Zeits. f. Physik* **34**, 232 (1925); J. Kuhne, *Zeits. f. Physik* **84**, 722 (1933); N. Wright and H. M. Randall, *Phys. Rev.* **44**, 391 (1933); Barnes, Benedict and Lewis, *Phys. Rev.* **47**, 918 (1935).

⁵ Randall, Dennison, Ginsberg and Weber, *Phys. Rev.* **52**, 160 (1937) (this paper will hereafter be referred to as RDGW).

water vapor and to analyze these data to obtain the rotational energy levels of the ground state of the D_2O molecule. The "far infra-red" is the term used generally for the region beyond about 20μ . At this point the prisms of the prism spectrographs become opaque to the long wave-length radiation and recourse must be made entirely to grating spectrographs. For molecules with small moments of inertia, such as NH_3 , HCl , and H_2O , the pure rotation frequencies are large enough to be located almost entirely on the short wave-length side of 100μ . For heavy molecules, on the other hand, the rotational frequencies are so small that the detection of their positions depends on data from the wave-length region beyond 100μ , a region which is as yet little explored under good dispersion since the energy concentrated in this region is so small.

The molecule of heavy water vapor is, as far as moments of inertia are concerned, a borderline molecule. It may be investigated while not completely, yet possibly with worthwhile results if the analysis is pushed to as long wave-lengths as it is possible to reach. This spectral examination must be at the same time of high enough resolution to separate the spectrum so that most of the lines may be clearly determined, experience with ordinary water vapor having shown that high resolution and dispersion are essential if the data obtained are to be used as the basis for a theoretical analysis.

II. EXPERIMENTAL

1. Experimental difficulties

The instrument used was a far infra-red grating spectrograph equipped with automatic recording mechanism and with an evacuable radiation path. This spectrograph and its predecessors have been rather completely described in the literature,⁶ and for this reason no further reference will be made here to its general features. The experimental problems which came up during the research fell mainly under four divisions: lack of energy, overlap of spectral orders, irregularity of deflections, and contamination of the substance under investigation. A brief paragraph concerning each of these problems follows.

⁶ H. M. Randall, *Rev. Sci. Inst.* **3**, 196 (1932); H. M. Randall, *Rev. Mod. Phys.* **10**, 72 (1938); H. M. Randall and F. A. Firestone, *Rev. Sci. Inst.* **9**, 404 (1938).

a. Lack of energy.—The form of the Planck energy distribution curve for radiation from a blackbody is well known. It shows a tremendous tailing off on the long wave-length side. For this long wave-length region the Rayleigh-Jeans equation, $E_\lambda d\lambda = C\lambda^{-4}kTd\lambda$, is a good first approximation. A study of this equation shows, for example, that the energy given off from a blackbody source in the 50μ region, though itself very small compared to the total radiation, is 16 times as great as that at 100μ and 256 times that at 200μ . Such an illustration gives a rough idea of the energy diminution with increase in wave-length, even though the source used, an electrically heated platinum strip coated with thorium oxide, had a more favorable energy distribution in this region than a blackbody would have.

Furthermore the problem was to examine this long wave-length region under high dispersion, that is with finely ruled gratings and narrow slits. (The "effective slit width" used in this research varied from 0.2 cm^{-1} to 0.5 cm^{-1} depending on the region.) This "spreading out" of the energy added materially to the smallness of the energy coming through the final slit to the thermopile. Indeed, beyond 150μ the radiant energy was found to be almost negligibly small when the spectrum was examined at the dispersion required. To work at all in this borderline region of small energy between 100μ and 150μ it was necessary to keep the spectrograph in almost perfect adjustment to exclude energy deficiencies which were not intrinsic. In this connection mention of the over-all sensitivity of the spectrograph may be interesting. Calculations based on Cartwright's thermopile equations⁷ indicated that 0.036 erg/sec. of radiant power delivered to the thermopile receivers would cause a deflection (at the recording camera drum) of 400 mm during one period (16 seconds) of the galvanometer. This deflection is 100 times that of the Brownian motion background and thus is measurable within an accuracy of one or two percent.

b. Overlapping spectral orders.—Six different agents contributed to the purification of the radiation, namely: the construction of the grating, and the materials out of which were made

⁷ C. H. Cartwright, *Zeits. f. Physik* **92**, 153 (1934).

TABLE I. Purification of radiation. Tests for presence of 2nd- or 3rd-order background radiation were made by introducing filters which cut out all 1st order in that region, but which pass the higher orders: in 20–30 μ region, use 2 mm NaCl; in the 27–60 μ region, use 2 mm KBr; and in 55–100 μ region, use 0.4 mm KI.

SPECTRAL REGION	SHUTTER	reststrahlen	FILTERS	
			PAR-AFFIN	CRYSTAL-LINE QUARTZ
18–23 μ	CaF ₂	mirror	2 mm	
22–36 μ	NaCl	CaF ₂ or NaF	2 mm	
25–40 μ	KCl or NaCl	NaF or CaF ₂	4 mm	
40–70 μ	KBr or KCl	mirror	4 mm	1 mm
65–85 μ	KI	KBr	4 mm	1 mm
80–100 μ	KI	KI	4 mm	2 mm
100–125 μ	KI	TlBr	4 mm	3 mm
120–160 μ	KI	TlI	4 mm	3 mm

the source, the thermopile receivers, the shutter, the *reststrahlen* plate, and the filters. The first three factors mentioned were more or less fixed throughout the research. Echelette gratings were used. These may be so designed that the greater part of the first-order energy is concentrated in a narrow region of the first-order spectrum, called the "blaze." All higher orders are present, overlapping the desired radiation, this being especially true in the blaze. For this reason measurements were made in regions at some distance from the grating blaze. Certain apparently unpredictable differences in design gave some gratings a higher percentage of the total energy in the first-order spectrum than other gratings.

The thorium-oxide-coated source proved to be the most satisfactory emitter over the whole region. The thermopile receivers were made either of Aquadag (graphite) coated on tinfoil,⁸ or of glass powder dusted over a thin glass receiver backed by an evaporated metal layer.⁹ Both types of receivers appeared to work equally well in the long wave-length region, though only qualitative comparisons were made between them.

The latter three factors were varied with the different wave-length regions desired. Table I gives the different combinations found most satisfactory in obtaining pure radiation. Very pure spectra could be obtained with these com-

⁸ N. Wright, Doctoral Thesis (U. of Mich., 1933); F. A. Firestone, *Rev. Sci. Inst.* **1**, 630 (1930).

⁹ C. H. Cartwright and J. Strong, *Procedures in Experimental Physics* (Strong, Editor) (Prentice-Hall, 1938) pp. 321. G. B. B. M. Sutherland, *Infra Red and Raman Spectra* (Methuen, 1935), p. 7.

binations up to 100 μ . Beyond that wave-length good results were obtained with certain gratings and poor results with others. It should be mentioned that the window for the evacuated thermopile was made of paraffin and has been counted in as a filter in the table.

c. Irregularity of deflections.—A great deal of time was spent in tracking down causes for the occasional irregular periods of deflection which made measurements of absorption minima either very inaccurate or quite impossible in the region of disturbance, as well as spoiling the aesthetic appeal of the entire record! Aside from occasional mechanical vibration disturbances and direct electrical effects, the main trouble was eliminated finally by enclosing the primary galvanometer in an airtight steel case, and by putting a radiofrequency choke across the thermopile-to-galvanometer leads. The latter was installed to eliminate heating and rectifying effects in the thermopile due to pick-up of high frequency oscillations from the cyclotron power units in the neighborhood.

d. Contamination of the D₂O vapor.—The absorption cell available for work with this spectrograph was a cylindrical Pyrex cell, 20 inches long and 11 inches in diameter, containing a 10-inch focusing mirror (with gold mirror surface) which was supported at one end of the cell on a chromium plated adjustable mounting. The cell ends were heavy glass disks which were sealed to the cylinder with rubber cement and rubber splicing tape. The seals, source to cell, and cell to spectrograph case, were likewise made with this rubber tape. Crystalline quartz served as window material for the cell in the spectral region beyond 40 μ . From 20 μ to 40 μ quartz is opaque, so an organic plastic called "Metastylene"* was used. This plastic was sufficiently transparent throughout this region (a broad absorption at 27 μ was too weak to be serious), but it warped, cracked, and melted under heat and pressure, so that windows had to be replaced frequently. It could not be used at all between the source and the cell, so for most of this work the glowing metal strip was in contact with the vapor in the absorption cell.

The cell had a radiation path of 90 cm. The usual procedure was to introduce enough D₂O

* Trade name for a commercial polystyrene

liquid into the cell so that it would, upon evaporation, fill the cell with saturated vapor (16 to 18 mm pressure on a mercury manometer) at room temperature. In some regions a longer absorption path would have been desirable if longer cells had been available. Calculations showed that 1 cc of D₂O liquid should be sufficient to saturate the cell volume. In actual practice 2 cc of D₂O were generally used in order to obtain the desired vapor pressure, for apparently a great deal of the D₂O was adsorbed on the cell walls.

Further evidence of this adsorption came from the observation that if the cell were well evacuated after having previously been full of air containing its usual amount of atmospheric H₂O vapor (the main spectrograph case is here assumed to be well evacuated at all times), the background energy records showed little if any trace of even the strongest H₂O absorption lines. Upon introducing a gram of D₂O (99.5 percent pure), immediately strong H₂O lines would appear in the spectrum as well as the expected D₂O lines, the former presumably being due mainly to the presence in the radiation path of H₂O molecules which had been dislodged from the cell walls upon impact from the freshly introduced D₂O molecules. Exchange phenomena, too, were undoubtedly present, resulting finally in an equilibrium mixture of H₂O, HDO, and D₂O molecules.

It was only after great pains were taken to dry the mirror, its mountings, and the interior walls of the absorption cell that a comparatively pure D₂O spectrum could be obtained upon introduction of the gram of D₂O. Ideally a cell is dried out by long baking at a temperature of 300 to 400 degrees centigrade. Such a procedure was impossible in this case since neither the cell walls, the windows, or the seals could stand such a high temperature. The method finally adopted for drying out this cell and introducing the D₂O vapor was about as follows: Gas from a cylinder tank of especially dried nitrogen, after being further dried by passing through three bubble bottles filled with fresh concentrated sulfuric acid and then through two large liquid-air traps, was introduced slowly into the previously evacuated cell until atmospheric pressure of nitrogen was obtained. A small stream of gas was then, for a six-hour period, allowed to pass through the cell, emerging from a second opening. The gas inlet then being closed, the cell was continuously evacuated by the Megavac pump for a second six-hour period. Throughout this 12-hour period the cell itself was heated to a temperature of 50 to 60°C to aid the drying out process by increasing the vapor pressure of the adsorbed vapor. This whole process of flushing with dried nitrogen followed by sustained evacuation under continuous gentle heating was repeated three or

TABLE II. Frequencies attributed to HDO. Symbolism used in this table has the following significance: × = definitely HDO (no H₂O or D₂O lines fall in this region at all); · = very weak H₂O or D₂O lines overlap the HDO line; ? = possibly due to higher spectral order; 2 = probably 2nd-order absorption line. (A blank space indicates that there are H₂O or D₂O lines superposed on the HDO enough so that the assignment is somewhat questionable.) (The intensity symbols are explained in a later paragraph.)

419.62 × mS	232.38 mw	179.88 × m	157.52 mS	136.70 × m
397.56 × mS	224.89 × m	177.62 m	156.47 × S	135.77 × mS
393.38 × S	218.08 × w	176.07 · m	153.55 S	135.22 × mS
368.88 × m	216.05 × mS	175.11 m	151.53 m	134.32 · S
360.46 × m	215.04 mw	172.28 m	150.56 mw	131.90 m
356.19 × m	213.67 · mS	171.63 m	150.10 × m	129.88 × m
345.10 × m	212.50 m	170.35 mS	149.10 mS	125.80 × m
340.74 × mS	210.88 × m	169.30 · S	148.65 m	124.67 mw
334.90 × mS	209.75 × m	167.19 × m	147.65 × m	122.82 m
331.30 · mS	206.40 m	166.46 · S	147.06 mS	119.58 · mS
330.31 mw	205.70 mw	165.25 m	145.90 × mS	118.86 m
305.18 mw	197.10 m	164.10 mw	145.08 m	118.70 × S
298.75 m	193.48 mw	163.50 m	144.53 · S	117.12 × m
270.70 × mS	190.42 × mw	163.28 · S	142.10 m	116.61 m
259.18 S	189.86 × m	162.42 m	141.50 mw	116.15 ?2m
250.15 × mS	187.43 × mw	161.68 mw	141.21 mw	115.40 S
246.95 × mS	185.94 × m	160.28 m	140.66 m	114.48 × ? S
246.42 × mw	184.70 mS	159.64 m	139.80 mS	113.93 × ? S
237.82 × mS	182.33 × m	158.93 m	138.95 m	113.19 × ?2 S
	180.39 × m	157.85 mS	137.16 × mS	111.78 × ?2 S
				110.73 × ?2 S

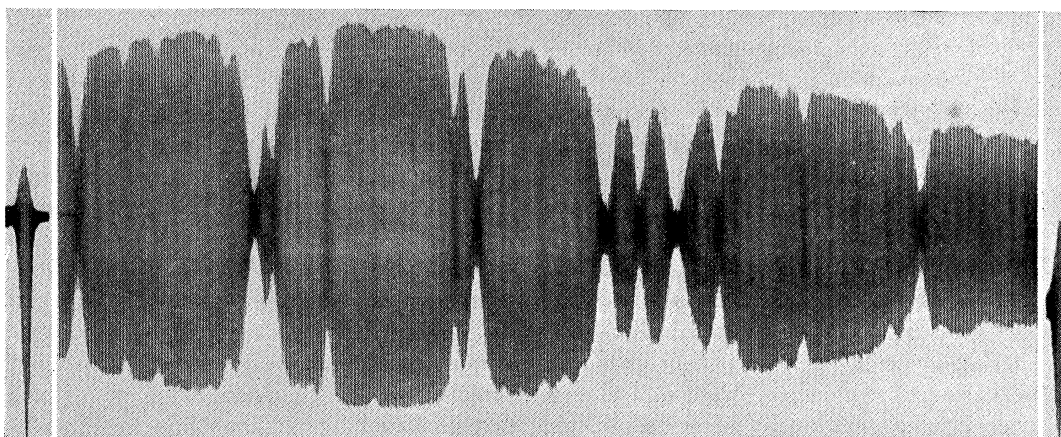


FIG. 1. H₂O vapor absorption in the region between 31 μ and 38 μ , using an echelette grating with 600 lines per inch (total number of lines is 12,000), low temperature source, amplification factor of $\times 200$, path length equivalent to 60 cm of saturated H₂O vapor at room temperature, effective slit width of 0.3 cm⁻¹. The dispersion is rather good in this record, as the "true width" of a strong absorption line is roughly four times the effective slit width. (Lines 0.5 cm⁻¹ apart were separated but two strong doublets of 0.25 cm⁻¹ separation distance look single.) The resolution is excellent. Optical path consists of thorium-oxide-coated source, Aquadag-coated thermopile receivers, NaF *reststrahlen* plate, NaCl shutter, 1 mm Metastyrene and 4 mm paraffin wax as filters. This arrangement gave excellent purity as is evidenced by the almost complete absorption of the stronger lines.

four times. Several one gram samples of D₂O liquid were then introduced into the cell, the heating and evacuation process being applied between each sample to further eliminate any remaining H₂O and to replace it by D₂O.

The final heavy water sample introduced was usually two grams. The D₂O reservoir flask was subjected to the same drying procedure. The liquid was introduced into it while dried nitrogen was being steadily passed through it. The reservoir was then attached to one of the cell inlets, and the D₂O vapor forced into the cell by gently heating the flask to quicken the evaporation process into the evacuated cell.

A rather complete transition from pure H₂O spectrum through a mixed H₂O, HDO, and D₂O spectrum to a pure D₂O spectrum was observed by making records of consecutive samples of supposedly pure D₂O introduced during different stages of the drying process. Indeed, the data on the HDO spectrum, which are given in Table II, were obtained from a critical comparison of such a series of transition spectra, and observation of which absorption lines disappeared at both ends of the spectral purity sequence.

2. Samples of records made

A large number of records of all kinds were made during the course of the work. While the

majority of them were made with D₂O in the absorption cell, a complete set of background records were made, as well as a set of H₂O records. All regions of the D₂O spectrum from 23 μ to 135 μ were covered at least twice and sometimes as many as six or eight times. Records made with different gratings were taken so as to overlap as much as possible to check the mutual consistency of the gratings. The grating ruled with 900 lines-per-inch was used over the region from 22 μ to 40 μ , the 600-line-per-inch grating from 26 μ to 60 μ , the 360-line grating from 45 μ to 100 μ , the 133-line grating from 65 μ to 135 μ , and the 87.8-line grating from 80 μ to 200 μ . Three other gratings were also used for supplementary work.

Two records are reproduced here with a linear reduction factor of $\frac{1}{6}$ (see Figs. 1 and 2) and details in connection with them will be found under the figures. They do not give a complete picture of the types of records which may be taken on the spectrograph used, and for other illustrations of records reference may be made to previously published articles.¹⁰

3. Results of the experimental work

The 210 experimentally determined D₂O fre-

¹⁰ Other records of D₂O and H₂O which were made during the course of this investigation may be found already published as follows: Randall and Firestone, reference 6, Figs. 5a, b, c, e, f, g.

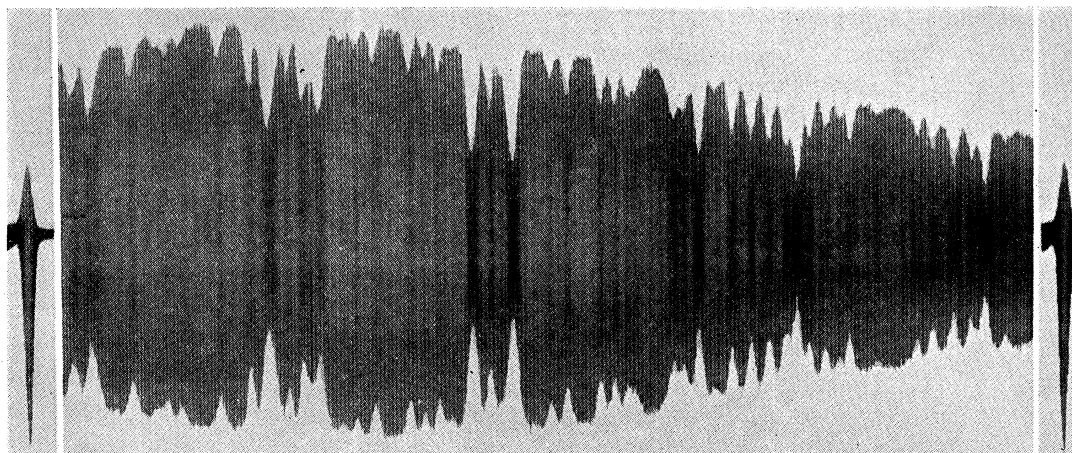


FIG. 2. D_2O vapor absorption in the same region and under identical conditions used for the H_2O record shown in Fig. 1. A comparison of the two records reveals that the D_2O lines are much weaker and much more numerous. The weakness is due partly to the fact that the D_2O transitions here recorded are between energy levels having higher quantum numbers than those for the H_2O record, and partly to the intrinsically greater strength of the H_2O absorptions. The greater number is a result of the greater mass of the molecular components of D_2O which cause a crowding together of all the energy levels.

quencies obtained from the absorption records, together with their respective estimated intensities have been tabulated in Table III. These frequencies, and the HDO frequencies in Table II, are vacuum frequencies since the radiation path was well evacuated at all times. The relative intensity symbols have the following significance: vvw (exceedingly weak) corresponds to from 0 percent to 5 percent absorption; vw (very weak) corresponds to from 5 percent to 10 percent; w (weak), 10 percent to 15 percent; mw (medium weak), 15 percent to 25 percent; m (medium), 25 percent to 40 percent; mS (medium strong), 40 percent to 55 percent; S (strong), 55 percent to 75 percent; and VS (very strong), 75 percent to 100 percent.

This research formed the first complete test of the recording spectrograph. For this reason it is interesting to notice the accuracy obtained for the frequency and intensity determinations. The latter are rough at best, as the instrument is not adapted for making simultaneous determinations of the energy background profile and the desired absorption curve. So many different optical path arrangements were used that such changes often changed the total energy background and the shape of this background. It will, however, be possible to install calibrated energy standards which will enable one to get rather high accuracy

for the relative and absolute intensities without the need for simultaneous background determinations.

The accuracy of the frequency determinations was uniformly excellent over the whole range. In the regions of high accuracy and good dispersion for each grating the frequencies could be determined within an average uncertainty of 0.05 cm^{-1} . The gratings available were of sufficient number and of proper line spacing and blaze angle characteristics to give such accuracy over the entire range from $20\ \mu$ to $180\ \mu$, assuming spectral purity in the first order. A great many retakes of different regions in the D_2O spectrum gave ample opportunity to check this stated accuracy. Absorption lines 0.5 cm^{-1} apart were partially resolved with ease, and under ideal conditions lines 0.3 cm^{-1} apart were detected as separate.

An interesting further check on the accuracy of the instrument was to compare the results obtained for H_2O with results previously obtained in this laboratory on a nonrecording spectrograph. One specific case will be cited. The vacuum values of measured frequencies of the twelve strongest single lines from the H_2O record reproduced in Fig. 1 were compared with the averaged data obtained on this hand operated

instrument.* (The weaker lines in the Fig. 1 record were not picked up in the earlier work.) The frequencies of Fig. 1 average 0.03 cm^{-1} higher than the RDGW values, a difference which is easily accounted for by the 0.05 cm^{-1} average uncertainty in the frequency determinations.

* This data is given in reference 5. The frequencies as tabulated in that paper, however, must be reduced to vacuum frequencies before they can be compared to those obtained from Fig. 1. Such a reduction diminishes each RDGW frequency by 0.03 percent (about 0.08 cm^{-1} on the average).

III. THEORETICAL

The problem now remains to identify the experimental absorption lines and from this identification to determine the rotational energy levels of the D_2O molecule.

1. Calculation of the "key" rotational energy levels

a. *The energy level equations.*—No attempt shall be made here to give a quantum theoretical derivation for the rotational energy levels, selection rules, and transition intensities of the asym-

TABLE III. The rotation frequencies of heavy water vapor.

Legend: $x = \nu/c_{\text{calc}}$ uncertain (no comparison key). $xx = \nu/c_{\text{calc}}$ very uncertain. $? = I_{\text{calc}}$ is uncertain. $* = \nu/c_{\text{obs}}$ is uncertain; may be spurious. $a = \nu/c_{\text{calc}}$ is uncertain because of the overlapping of strong lines.

ν/c_{OBS}	I_{OBS}	ν/c_{CALC}	I_{CALC}	$j''_1 j''_2 - j''_1 j''_2$ (ASSIGNED TRANSITION)	ν/c_{OBS}	I_{OBS}	ν/c_{CALC}	I_{CALC}	$j''_1 j''_2 - j''_1 j''_2$ (ASSIGNED TRANSITION)	ν/c_{OBS}	I_{OBS}	ν/c_{CALC}	I_{CALC}	$j''_1 j''_2 - j''_1 j''_2$ (ASSIGNED TRANSITION)		
386.63	w				277.11	S	277.11	8	11 ₇ - 10 ₅	220.30	S	220.50 a	1.3	8 ₋₃ - 7 ₋₇		
383.70	w								11 ₈ - 10 ₆			220.26	8	11 ₋₁ - 10 ₋₃		
378.72	vw				275.38	mS	275.4 xx	8	12 ₄ - 11 ₂			220.26	26	10 ₂ - 9 ₀		
372.67	mw								12 ₃ - 11 ₃			219.47	13	10 ₁ - 9 ₁		
361.20	w				274.44	mS		.6	10 ₋₅ - 9 ₋₉	219.52	m					
358.36	m				273.48	mS	273.62			216.05	m					
354.40	mw				272.65	mS				213.80	m					
351.30	mw				272.12	S				212.42	w	212.55 ?	3	7 ₀ - 6 ₋₄		
348.36	w	348.61 ?	2.0	11 ₀ - 10 ₋₄	271.52	m	271.5 xx	4	13 ₁ - 12 ₋₁	211.35	mS	211.4 xx	4.5	12 ₋₃ - 11 ₋₃		
346.10	w								13 ₀ - 12 ₀			211.35	mS	211.35	68	8 ₅ - 7 ₄
343.50*	mw	343.67 ?	1.0	10 ₁ - 9 ₋₃	269.94	w						208.00	20	9 ₃ - 8 ₁		
339.50	m				269.51	m	269.50 ?	2	8 ₁ - 7 ₋₃	207.88	mS	207.88	38	9 ₂ - 8 ₁		
337.70	mw				268.18	w				206.55	mw	206.55	17	11 ₋₂ - 10 ₋₂		
333.88	w				265.54	m	265.50 ?	1	10 ₋₃ - 9 ₋₇	205.59	m	205.62	29	10 ₀ - 9 ₋₂		
331.30	w				264.56	m	264.56	15	10 ₈ - 9 ₆	203.90	m					
330.21	vw								10 ₇ - 9 ₇	202.80	mw	202.80 ?	6	10 ₋₂ - 9 ₋₄		
328.90	w				263.75	mw	263.80	1.5	10 ₋₆ - 9 ₋₈	201.60	vw					
326.25	mw						263.65 ?	4	7 ₂ - 6 ₋₂	200.44	m					
324.88	vw	324.9 xx	.8	12 ₁₂ - 11 ₁₀ 12 ₁₁ - 11 ₁₁	263.11	mS	263.11	13	11 ₅ - 10 ₃			199.50 a?		6 ₁ - 5 ₋₃		
									11 ₄ - 10 ₄	199.45	m	199.40 a	2.5	8 ₋₄ - 7 ₋₆		
					262.18	w				198.78	mS	198.78	96	7 ₁ - 6 ₅		
					260.19	S	260.2 x	8	12 ₂ - 11 ₀			198.75 a	8	7 ₆ - 6 ₆		
									12 ₁ - 11 ₁			198.56 a	13	9 ₋₃ - 8 ₋₅		
					259.18	mS						198.56 a	13	10 ₋₁ - 9 ₋₁		
					258.23	mw	258.28	.6	11 ₋₅ - 10 ₋₇	197.18	m					
					257.37	m				195.64	S	195.65	54	8 ₄ - 7 ₂		
					256.95	mS						195.61	27	8 ₃ - 7 ₈		
					255.00	m	254.93 ?		6 ₃ - 5 ₋₁	194.74	m	194.72	3.5	7 ₋₂ - 6 ₋₆		
					254.00	mw	254 xx?	1.8	12 ₋₄ - 11 ₋₆	194.28	mw					
					252.09	m	252.09	* 21	9 ₉ - 8 ₇	192.15	mS	192.10	22	9 ₁ - 8 ₋₁		
									9 ₈ - 8 ₈			189.42 ?		5 ₂ - 4 ₋₂		
					250.80	m	250.80	22	10 ₆ - 9 ₄	189.28	mS	189.26	43	9 ₀ - 8 ₀		
									10 ₅ - 9 ₅	188.28	mw					
					250.15	mw				186.22	w					
					249.55	w				184.69	S					
					248.77	w						183.43	36	7 ₅ - 6 ₃		
							248.10 a	6	11 ₃ - 10 ₁	183.42	VS	183.42	72	7 ₄ - 6 ₄		
					248.07	m	248.03	12	11 ₂ - 10 ₂			183.20 a	20	9 ₋₁ - 8 ₋₃		
							245.5 xx	7	12 ₀ - 11 ₋₂	181.55	m					
					245.10	mS	245.39 ?	2	9 ₋₂ - 8 ₋₆	179.37	S	179.37	60	8 ₂ - 7 ₀		
							244.96	2	9 ₋₄ - 8 ₋₈	178.32	S	178.32	30	8 ₁ - 7 ₁		
					244.17	mS				177.72	mw					
					241.35	mw	241.3 xx	3	12 ₋₁ - 11 ₋₁	176.93	w					
					238.38	mS	238.38	30	9 ₇ - 8 ₅	176.19	m	176.2 xx	5.5	12 ₋₅ - 11 ₋₅		
									9 ₆ - 8 ₆	175.15	w					
					237.47	m				173.58	mS					
					235.96	m	235.97	20	10 ₄ - 9 ₂			172.65 a	2	6 ₋₁ - 5 ₋₅		
							235.95	10	10 ₃ - 9 ₃	172.37	mS	172.37 ?	20	8 ₋₂ - 7 ₋₄		
					232.52	m	232.50 ?	1	9 ₋₅ - 8 ₋₇	171.66	m					
							232.42	8	11 ₁ - 10 ₋₁	170.81	VS	170.81	142	6 ₆ - 5 ₄		
					231.50	w	231.5 xx	10	12 ₋₃ - 11 ₋₄							
					230.93	w	230.98	15	10 ₋₄ - 9 ₋₆	169.88	vw					
					228.90	mS	228.90 ?	4	8 ₋₁ - 7 ₋₅	169.32	mS	169.30	17	7 ₋₃ - 6 ₋₅		
							227.18 ?	2	10 ₋₄ - 9 ₋₆	168.40	m					
					225.94	m	225.94	45	8 ₈ - 7 ₆			166.88	38	7 ₃ - 6 ₁		
									8 ₇ - 7 ₇			166.76	50	8 ₀ - 7 ₋₂		
							225.94 ?	2	11 ₋₃ - 10 ₋₅	166.67	VS	166.75 a	14	10 ₋₃ - 9 ₋₃		
					223.71	mS	223.71	16	9 ₅ - 8 ₃	166.60		166.60	77	7 ₂ - 6 ₂		
							223.70	32	9 ₄ - 8 ₄							
					221.41	w				165.25	vw					
										164.15	w					

TABLE IV. Ground state rotational energy levels of the heavy water vapor molecule.

$W-W_k$	SYM	j_τ	W	$W-W_k$	SYM	j_τ	W	$W-W_k$	SYM	j_τ	W	$W-W_k$	SYM	j_τ	W
0.0	++	0 ₀	0.00	.24	++	6 ₋₂	308.69	2.74	-+	9 ₋₁	708.80	1.89	-+	11 ₋₇	876.94
				.97	-+	6 ₋₃	288.20	2.32	++	9 ₋₂	703.03	1.48	++	11 ₋₈	794.33
.0	+-	1 ₁	22.63	.88	--	6 ₋₄	279.68	1.89	+-	9 ₋₃	659.20	1.46	+-	11 ₋₉	793.96
.0	--	1 ₀	20.20	.18	+-	6 ₋₅	232.60	1.15	--	9 ₋₄	632.68	1.39	--	11 ₋₁₀	692.57
.0	-+	1 ₋₁	12.08	.06	++	6 ₋₆	231.92	2.32	-+	9 ₋₅	620.30	1.39	-+	11 ₋₁₁	692.57
								1.25	++	9 ₋₆	562.12				
.0	++	2 ₂	74.03	.33	+-	7 ₇	780.76	1.07	+-	9 ₋₇	560.45		++	12 ₁₂	2162.8
.02	-+	2 ₁	73.56	.33	--	7 ₆	780.76	1.03	--	9 ₋₈	479.85		-+	12 ₁₁	2162.8
.0	--	2 ₀	49.20	.91	-+	7 ₅	668.83	1.02	-+	9 ₋₉	479.80		--	12 ₆	1668.15
.0	+-	2 ₋₁	41.94	.91	++	7 ₄	668.83						+-	12 ₅	1668.15
.0	++	2 ₋₂	35.75	1.26	+-	7 ₃	572.37	-2.02	++	10 ₁₀	1536.09		++	12 ₄	1526.35
				1.26	--	7 ₂	572.34	-2.02	-+	10 ₉	1536.09		-+	12 ₃	1526.35
.03	+-	3 ₃	156.46	1.36	-+	7 ₁	493.18	.17	--	10 ₈	1383.12		--	12 ₂	1400.0
.04	--	3 ₂	156.43	1.26	++	7 ₀	492.23	.17	+-	10 ₇	1383.12		+-	12 ₁	1400.0
.0	-+	3 ₁	112.02	1.21	+-	7 ₋₁	436.15	1.64	+-	10 ₆	1242.49		++	12 ₀	1287.55
.0	++	3 ₀	109.81	.52	--	7 ₋₂	426.64	1.64	-+	10 ₅	1242.49		-+	12 ₋₁	1287.5
.0	+-	3 ₋₁	88.76	1.82	-+	7 ₋₃	402.00	2.46	--	10 ₄	1115.45		--	12 ₋₂	1191.8
.30	--	3 ₋₂	74.58	.51	++	7 ₋₄	368.78	2.46	+-	10 ₃	1115.45		+-	12 ₋₃	1190.75
.0	-+	3 ₋₃	70.24	.95	+-	7 ₋₅	364.12	2.37	++	10 ₂	1002.92		++	12 ₋₄	1136.25
				.44	--	7 ₋₆	305.32	2.38	-+	10 ₁	1002.87		-+	12 ₋₅	1107.8
.04	++	4 ₄	269.04	.47	-+	7 ₋₇	305.10	2.86	--	10 ₀	908.65		--	12 ₋₆	1081.65
.04	-+	4 ₃	269.03					2.86	+-	10 ₋₁	907.36		+-	12 ₋₇	1022.15
.21	--	4 ₂	206.14	.16	++	8 ₈	1006.70	2.13	++	10 ₋₂	835.48		++	12 ₋₈	1019.15
.25	+-	4 ₁	205.76	.16	-+	8 ₇	1006.70	2.19	-+	10 ₋₃	825.95		-+	12 ₋₉	925.15
.25	++	4 ₀	164.03	1.05	--	8 ₆	880.18	2.75	--	10 ₋₄	791.02		--	12 ₋₁₀	924.95
.52	-+	4 ₋₁	158.29	1.05	+-	8 ₅	880.18	2.84	-+	10 ₋₅	753.42		+-	12 ₋₁₁	813.35
.77	--	4 ₋₂	141.42	1.60	++	8 ₄	767.99	1.67	++	10 ₋₆	743.65		++	12 ₋₁₂	813.35
.41	+-	4 ₋₃	117.37	1.60	-+	8 ₃	767.98	1.31	-+	10 ₋₇	673.32				
.08	++	4 ₋₄	114.71	1.70	--	8 ₂	671.60	1.64	--	10 ₋₈	672.92		-+	13 ₃	1688.5
				1.75	+-	8 ₁	671.50	1.29	+-	10 ₋₉	581.52		++	13 ₂	1688.3
.21	+-	5 ₅	411.18	1.34	++	8 ₀	593.40	1.30	++	10 ₋₁₀	581.51		+-	13 ₁	1559.0
.22	--	5 ₄	411.18	1.48	-+	8 ₋₁	591.30						--	13 ₀	1559.0
.33	-+	5 ₃	330.89	1.09	--	8 ₋₂	541.15	-4.45	+-	11 ₁₁	1837.89		--	13 ₋₈	1171.85
.32	++	5 ₂	330.84	2.34	+-	8 ₋₃	525.60	-4.45	--	11 ₁₀	1837.89		++	13 ₋₁₀	1065.25
.88	+-	5 ₁	269.34	1.00	++	8 ₋₄	504.72	-1.68	-+	11 ₉	1672.71		+-	13 ₋₁₁	1065.45
.45	--	5 ₀	267.41	.87	-+	8 ₋₅	460.45	-1.68	++	11 ₈	1672.71		--	13 ₋₁₂	943.75
1.05	-+	5 ₋₁	230.47	.93	--	8 ₋₆	457.64	1.14	+-	11 ₇	1519.60		-+	13 ₋₁₃	943.75
.46	++	5 ₋₂	217.47	.75	+-	8 ₋₇	387.80	1.14	--	11 ₆	1519.60				
1.57	+-	5 ₋₃	205.99	.78	++	8 ₋₈	387.72	2.45	-+	11 ₅	1378.56		++	14 ₂	1858.8
.24	--	5 ₋₄	169.96					2.45	++	11 ₄	1378.56		-+	14 ₁	1858.8
.34	-+	5 ₋₅	168.88	-0.55	+-	9 ₉	1258.79	2.72	+-	11 ₃	1250.97		-+	14 ₋₁₁	1215.2
				-0.55	--	9 ₈	1258.79	2.70	--	11 ₂	1250.95		--	14 ₋₁₂	1215.0
.32	++	6 ₆	581.98	.87	-+	9 ₇	1118.56	3.56	-+	11 ₁	1139.78		+-	14 ₋₁₃	1083.8
.32	-+	6 ₅	581.98	.87	++	9 ₆	1118.56	3.49	++	11 ₀	1139.63		++	14 ₋₁₄	1083.8
.56	--	6 ₄	485.41	1.75	+-	9 ₅	991.69	2.96	+-	11 ₋₁	1046.21				
.57	+-	6 ₃	485.40	1.75	--	9 ₄	991.69	2.39	--	11 ₋₂	1042.03		++	15 ₋₁₂	1374.7
.96	++	6 ₂	405.74	2.15	-+	9 ₃	879.50	3.15	-+	11 ₋₃	979.36		+-	15 ₋₁₃	1374.8
.98	-+	6 ₁	405.49	2.15	++	9 ₂	879.48	2.84	++	11 ₋₄	960.32		--	15 ₋₁₄	1233.4
0.79	--	6 ₀	345.43	2.09	+-	9 ₁	783.40	1.21	+-	11 ₋₅	931.60		-+	15 ₋₁₅	1233.4
.89	+-	6 ₋₁	341.53	1.77	--	9 ₀	782.66	2.43	--	11 ₋₆	882.26				

b , there being four such equations for each value of j , and a total of $2j+1$ roots for each value of j . The energy levels for each j are arbitrarily arranged by order of magnitude and labeled with an index, τ , which runs from $+j$ to $-j$.

Energy levels through $j=11$ were calculated by means of these equations. They were then corrected for rotational stretching by a method to be described later. These corrected energy levels, hereafter called the key energy levels, are not listed in this paper explicitly, but may be

obtained from Table IV by subtracting from each member in column 4 the corresponding member of column 1. It remains to explain the basis for the choice of the moments of inertia, and the method of correcting for the rotational stretching effects. These two subjects will be considered in order.

b. Calculation of "reciprocal moments" of inertia.—The three principal moments of inertia of any rigid molecule may be computed by the equations of classical mechanics if the atomic

masses and interatomic distances are known. The masses in this case are well known, and the other atomic constants have been computed by Mecke¹⁴ for H₂O from experimental data. Assuming that the potential constants, which govern the interatomic distances, are independent of mass changes in the molecule, these H₂O values will also hold for D₂O. With Mecke's value for the atomic constants, r , and φ (see Fig. 3), the reciprocal moments for D₂O become; $A=15.15$ cm⁻¹, $B=7.21$ cm⁻¹, and $C=4.89$ cm⁻¹. (Note that these do not differ greatly from the values finally used.)

The D₂O molecule is, however, not a rigid rotator. It has vibrational modes and in the ground vibrational state, even for the case of no rotation, it has a certain amount of energy due to the everpresent vibrational half-quantum numbers. Since there is a vibration-rotation interaction, this gentle vibration of the molecule causes the moments of inertia for the ground state to differ from the "true" moments determined above.

The choice of the moments of inertia upon which to base the preliminary energy levels was crucial; they had to be very nearly correct if the identification was to be straightforward. The "true" moments were of the right order of magnitude, but it was decided to attempt to find a better set which would depend somewhat on this vibration effect. Mecke¹⁴ has evaluated the "effective" moments of inertia of H₂O for the ground state as well as for a number of the excited vibrational states from measurements of the vibration-rotation bands in the near infra-red. If the "isotope effect" upon the moments is known, the corresponding effective moments for D₂O may be found. The evaluation of this mass dependence for an asymmetric or even for a symmetric molecule would involve a great deal of analysis and computation. The process is known, however, for the simpler case of the diatomic molecule.¹⁵ If mass variations are assumed to affect the moments of inertia in the same way for various types of molecules, then an analogy will prove helpful.

The procedure followed was to find the zeroth-

order and the 2nd-order solutions of the diatomic molecule, then to determine what changes in the moments of inertia of the zeroth-order solution would give the results gotten straightforwardly by means of the more exact solution. Such computation gave the following expression

$$(\hbar^2/8\pi^2)(1/I_{\text{eff}}) = K_1 + K_2(n + \frac{1}{2}) + K_3j(j+1)$$

where the K 's are constants dependent on the true moment of inertia of the molecule (diatomic molecule has only one nonzero moment) and upon the normal frequency of vibration. The mass dependency only gives

$$1/I_{\text{eff}} = k\mu^{-1} + k'\mu^{-3}(n + \frac{1}{2}) + k''\mu^{-2}j(j+1),$$

where the k 's are constants which are independent of mass. (Dependence on vibrational state only is considered here. Rotational perturbation effects will be considered separately later. For this reason the last term on the right will be ignored.) Application of the analogy between the diatomic molecule and the asymmetric rotator molecule suggests that the effective reciprocal moments of the water vapor type molecule be written in the following form

$$A = a_0 + \sum_{i=1}^3 a_i(n_i + \frac{1}{2})$$

where $a_0 = k_0\mu^{-1}$, and $a_i = k_i\mu^{-3}$, with similar equations for B and C .

The 12 constants in the three H₂O equations of this type were so chosen that they gave a minimum deviation between the moments of inertia calculated by means of them and the moments

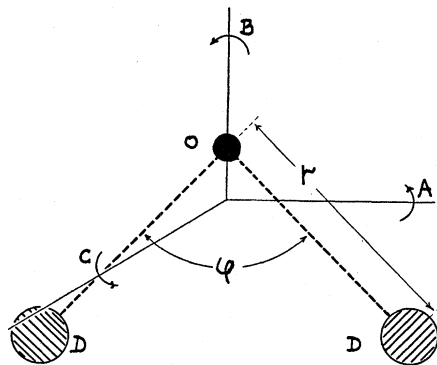


FIG. 3. Diagram of the D₂O vapor molecule, showing the dimensional quantities, r , and φ , and the axes of inertia, A , B , and C .

¹⁴R. Mecke, *et al.*, *Zeits. f. Physik* **81**, 313, 445, 465 (1933).

¹⁵W. F. Colby, *Phys. Rev.* **34**, 53 (1929); E. Fues, *Ann. d. Physik* **80**, 367 (1926).

determined by Mecke from the experimental data of his 17 most accurately located vibration bands. Since the constants for D₂O are related to those for H₂O as follows,

$$a_{0D} = \left(\frac{\mu_H}{\mu_D}\right)_A a_{0H}; \quad a_{iD} = \left(\frac{\mu_H}{\mu_D}\right)_A^{3/2} a_{iH}, \quad i=1, 2, 3$$

the effective reciprocal moments for D₂O may be determined by means of the following combined relation

$$A = \left(\frac{\mu_H}{\mu_D}\right)_A a_{0H} + \left(\frac{\mu_H}{\mu_D}\right)_A^{-3/2} \sum_{i=1}^3 a_{iH} \left(n_i + \frac{1}{2}\right)$$

(with similar expressions for *B* and *C*) if the value of the reduced mass ratios is known. This problem of choosing reduced masses for the asymmetric molecules presents an additional problem. Strictly speaking, the term "reduced mass" applies only to a two-body system. However if the analogy be drawn upon again, it is possible to make a choice of reduced masses associated with the moments of inertia about the two principal axes lying in the plane (*A* and *B*; see Fig. 3) which are quite unambiguous. For the reduced mass associated with the reciprocal moment, *C*, about the axis perpendicular to the molecular plane, different values could be obtained when calculated from different but perhaps equally valid points of view. It was finally decided to evaluate *C* for any particular vibration state by means of the classical relationship: $I_C = I_A + I_B$. This relation holds for any rigid plane figure but can only be an approximation for a vibrating plane molecule.

Table V gives the values of the inertial constants for H₂O and D₂O. They are of value for the calculation of reciprocal moments for vibration states other than the ground state. It was by means of these constants that the reciprocal moments finally used were evaluated.

c. The rotational stretching correction.—The perturbing action of rotation on the moments of inertia was not evaluated through the use of the diatomic molecule analogy as was done for the vibration-rotation interaction. An additional rotational quantum number is present, there being no parallel to τ or k in the diatomic case. Thus any computation of rotational correction based on this simpler molecule would be too incomplete

TABLE V. *Inertial constants.*

	H ₂ O	D ₂ O		H ₂ O	D ₂ O		H ₂ O	D ₂ O
<i>a</i> ₀	27.41	15.22	<i>b</i> ₀	14.56	7.28	<i>c</i> ₀	9.53	4.92
<i>a</i> ₁	-0.70	-0.29	<i>b</i> ₁	-0.24	-0.09	<i>c</i> ₁	-0.17	-0.06
<i>a</i> ₂	2.70	1.12	<i>b</i> ₂	0.22	0.08	<i>c</i> ₂	-0.17	-0.06
<i>a</i> ₃	-1.20	-0.50	<i>b</i> ₃	-0.10	-0.04	<i>c</i> ₃	-0.15	-0.06

to be valuable. This rotational perturbation upon the moments of inertia of the asymmetric rotator was a problem which had not been solved at the time this analysis was made. Yet it is a very important correction, having especially large influence upon light molecules. Qualitatively it differs for each value of *j* and τ , increasing rapidly for higher quantum numbers.

It was found more feasible to correct the energy levels themselves for rotation, rather than to attempt some correction directly to the reciprocal moments. Order of magnitude rotational corrections for the highest and the lowest energy levels of any particular *j* value might have been computed in the same manner that was done⁵ for H₂O. However since a complete list of the rotational corrections had been found⁵ for H₂O, it was more convenient to find how these correction factors depended on mass changes, and to apply this mass dependence ratio to get the D₂O factors from the H₂O factors. This dependency may easily be found from Dennison's zeroth-order rotational energy level correction development. He gives

$$\delta W_0/hc = \alpha j^4/\beta$$

where

$$\alpha = h/8\pi^2\mu y_0^2; \quad \beta = (ab - d^2)y_0^2/2b.$$

Therefore

$$\delta W_0 \sim \mu^{-2}; \quad \delta W_{0D} = (\mu_H/\mu_D)^2 \delta W_{0H}.$$

This discussion, for any given *j* value, applies (1) to rotation about the least axis of inertia (the 2 largest τ values) in which the mass factor is approximately 0.308; and (2), to a lesser approximation, to rotation about the greatest axis (the 2 smallest τ values) for which the mass ratio factor is about 0.268. Corrections for the energy levels between the highest and the lowest τ value pairs, for a given *j*, fitted in only roughly with this discussion of mass dependence. The conversion factor for them was assumed to lie some-

where between the two values given above. Thus for many of the corrections terms there was an uncertainty of 10 percent to 20 percent, assuming that the H_2O values to which the mass factors were applied were essentially correct. Rigorous analysis of the effect of rotation upon rotation must be made before this uncertainty is eliminated.

2. Intensities of the rotation lines

a. Relation between the τ and k index.—(This preliminary discussion of the relation between symmetric rotators and asymmetric rotators will prove valuable for reference later when line intensities are considered.) There is no direct relation between the index, τ , of the asymmetric rotator and the quantum number, k , of the symmetric rotator. However Dennison¹⁶ has shown that if for any particular value of j , the $2j+1$ values of W/hc are plotted for varying degrees of asymmetry (letting $I_A < I_B < I_C$, and letting I_B vary in value from I_A to I_C), in both limiting cases where the asymmetry disappears, single τ values or pairs of τ values may be associated with each of the k 's for the resulting symmetric rotator. Also each energy level retains its original τ index throughout as the ordering by magnitude does not change.

Further Dennison shows that an asymmetrical rotator, when in one of its closely paired energy states corresponding to its larger τ values, it is very similar to a symmetric rotator whose least moment of inertia lies along the unique axis (axis of rotation). The asymmetric rotator in these states, may, therefore, be qualitatively considered as rotating around its axis of least inertia. By the same reasoning an asymmetric rotator, when in energy states of lowest (large negative) τ values, can be best pictured as rotating around its greatest inertial axis. Levels corresponding to the intermediate values of the index, τ , are badly paired, and fit in poorly with either of the symmetric rotator cases considered. Therefore these levels are associated roughly with rotations about the intermediate moment of inertia axis, a case having no counterpart in the symmetric rotator.

b. Symmetry classes and selection rules.—Each wave function, $\psi_{j\tau}$, belongs to one of four sym-

metry classes, $(++)$, $(--)$, $(+-)$, and $(-+)$. The first sign in the bracket is determined by the symmetric rotator k number to which the τ index is associated when the asymmetric rotator is pictured as spinning about its axis of greatest inertia, being positive for even values of this k , and negative for odd values. The second sign is similarly positive or negative depending on the "even"ness or "odd"ness of the k value associated with the wave function's τ value for assumed rotation about the least moment of inertia axis. The reasons for this scheme of assignment are given in Dennison's paper¹⁶ together with a derivation of the following selection rules: (1) for j , $\Delta j = \pm 1, 0$; (2) for τ , if the electric moment lies along the middle moment of inertia axis (this being true of D_2O and H_2O in the ground state) transitions may occur only between $(++)$ and $(--)$, or between $(+-)$ and $(-+)$.

c. Transition probabilities and intensities.—Tolman¹⁷ gives a derivation of the expression for the intensity of an absorption transition in the general molecular case. Applying this to the special case of the D_2O molecule asymmetric rotator, the intensity of a transition from state $\psi_{j''\tau''}$ up to state $\psi_{j'\tau'}$ is given by

$$I_{j''\tau''}^{j'\tau'} \cong I_{j''k''}^{j'k'} = CF(\nu/c)BDA_{j''k''}^{j'k'}$$

C is a constant for any given molecule. It has the value

$$C = 4\pi^2 NM^2 / 3h \sum_{\alpha} g_{\alpha} e^{-W_{\alpha}/kT}$$

where M is the constant factor in the symmetric rotator electric moment matrix, N is the total number of molecules per cc, g_{α} is the statistical weight of the state with energy W_{α} .

F is the factor accounting for alternation of intensities due to nuclear spin contributions. For D_2O it takes on the values

$$F = \frac{2}{3} \text{ for even } \tau \text{ valued transitions} \\ F = \frac{1}{3} \text{ for odd } \tau \text{ valued transitions}$$

ν/c is the transition frequency expressed in cm^{-1} .

B is the Boltzmann factor accounting for the statistical distribution as a function of energy.

¹⁶ D. M. Dennison, Rev. Mod. Phys. **3**, 280 (1931). In this regard see especially Fig. 15 on page 322 of this reference.

¹⁷ R. C. Tolman, *Statistical Mechanics with Applications to Physics and Chemistry* (New York, 1927), p. 268.

As usual it is written $\exp[-W_{j''\tau''}/kT]$; for room temperature it has the value, when written in more convenient form,

$$B = \exp[-0.0049W_{j''\tau''}/hc].$$

D , the factor accounting for differences between induced absorption and induced coherent emission, has the value

$$D = 1 - e^{-h\nu/kT}.$$

The $A_{j''k''}^{j'k'}$ are factors in the symmetric rotator electric moment matrix which are dependent on the quantum numbers j and k . (They are also made to include the statistical weight factor, $2j+1$, introduced because of the energy expression being degenerate in the third quantum number, m .) Specifically, as calculated by Dennison,¹⁶

$$A_{j-1, k\mp 1}^{j, k} = \frac{(j\pm k)(j\pm k-1)}{j},$$

$$A_{j, k\mp 1}^{j, k} = \frac{(2j+1)(j\pm k)(j\mp k+1)}{j(j+1)}.$$

There are a number of important remarks still to be made in connection with this intensity expression. First of all a justification for the use of symmetric rotator elements in the intensity expression for an asymmetric rotator must be given. $A_{j''\tau''}^{j'\tau'}$ is the matrix element of the electric moment corresponding to the transition whose intensity is sought. It is to be calculated from the minors of the secular determinant constructed from the energy matrix of the asymmetric rotator. Dennison⁵ has calculated these matrix elements through $j=3$, and has shown that an easier method of getting the approximate intensities of the more important transitions is through the use of symmetric rotator elements. This can be shown qualitatively by recalling that wave functions of large τ index can be associated with rotation of the asymmetric rotator about its least inertial axis, and that corresponding energy levels may be approximated by energy levels of a symmetric rotator spinning about a comparable "least" axis. These approximations also hold good for the matrix elements of transitions between members within this class of wave functions. Thus the intensities of this class of

transitions may be well approximated by the intensities of the corresponding symmetric rotator transitions.

A like discussion shows that intensities of transition between levels of low τ index are fairly well approximated by intensities calculated for corresponding transitions of a symmetric rotator when spinning about its comparable axis of greatest inertia. The levels with intermediate τ indices being poorly approximated, a transition into this region or across this region must be computed from both "points of view," and some sort of weighted average taken which will give a rough idea of the line intensity. A large number of transitions allowed for the asymmetric rotator cannot be calculated in this approximate way as the selection rules forbid them in the case of the symmetric rotator. These lines will be ignored as they will be assumed to be too weak to be of importance in the identification of experimentally observed absorption lines.

Furthermore the evaluation of the constant, C , demands some notice. To compute absolute intensities the "zustande summa" for the D_2O molecule would have to be computed. This is impossible without previous knowledge of all the important energy levels. Relative intensities were accordingly used in this analysis. It was helpful to adjust the constant so that the D_2O intensities are on the same relative scale as the H_2O intensities of the RDGW study. The latter molecule's transition intensities have been tabulated⁵ assuming the C for H_2O to be unity. The constants C_H and C_D , differ only because of different masses. If the assumption is made that the effect of mass changes upon this constant is somewhat the same for different types of molecules, then it can be evaluated easily through the solution of the problem for the diatomic molecule. In this case,

$$W = \frac{j(j+1)h^2}{8\pi^2I}, \quad g_j = 2j+1$$

and the *zustande summa*

$$\sum_{j=0}^{\infty} (2j+1) \exp[-\{j(j+1)h^2/8\pi^2IkT\}].$$

Let $s = h^2/8\pi^2IkT$, and approximate the summation by an integral over j .

$$\int_0^{\infty} (2j+1)e^{-i(j+1)S}dj = \frac{1}{S} \int_0^{\infty} e^{-i(j+1)S}d(j(j+1)S) = \frac{1}{S} \sim \mu.$$

The *zustande summa* varies directly, and therefore the constant C , varies inversely with the reduced mass.

$$C_D\mu_D = C_H\mu_H; \quad C_D = (\mu_H/\mu_D)C_H; \quad C_H \equiv 1.$$

These mass ratios may be shown to take on values of 0.5, 0.555, and 0.543 depending upon which axis is chosen in computing the reduced masses. Since both the analogy and the calculation itself are only approximate, the value $C_D = 0.5$ has been used throughout the analysis.

Finally a word about the nuclear spin factor, F . The D_2O molecule contains two identical nuclei, deuterons, which obey Einstein-Bose statistics. Each has a nuclear spin of $\hbar/2\pi$. Alternating intensities are observed in the rotation spectra of such homonuclear molecules. The intensity of transition between symmetric levels divided by that between antisymmetric levels¹⁸ is for this case: $(S_n+1)/S_n = 2/1$. The $(++)$ and $(--)$ levels (even τ values) are symmetric, while the $(+-)$ and $(-+)$ levels (odd τ) are antisymmetric. For this analysis, then, we let $F = \frac{2}{3}$ for even- τ transitions, and $F = \frac{1}{3}$ for the odd.

3. The analysis

The records, as experimentally made, were photographic plots of intensity as the ordinate against *wave-length* as the approximately linear abscissa. Different records had widely different coordinate scale factors and were thus often difficult to compare with each other. For the purpose of study and analysis it was convenient to plot the average of these data on a linear *frequency* scale. This plot appears as the connected curve in Fig. 4.

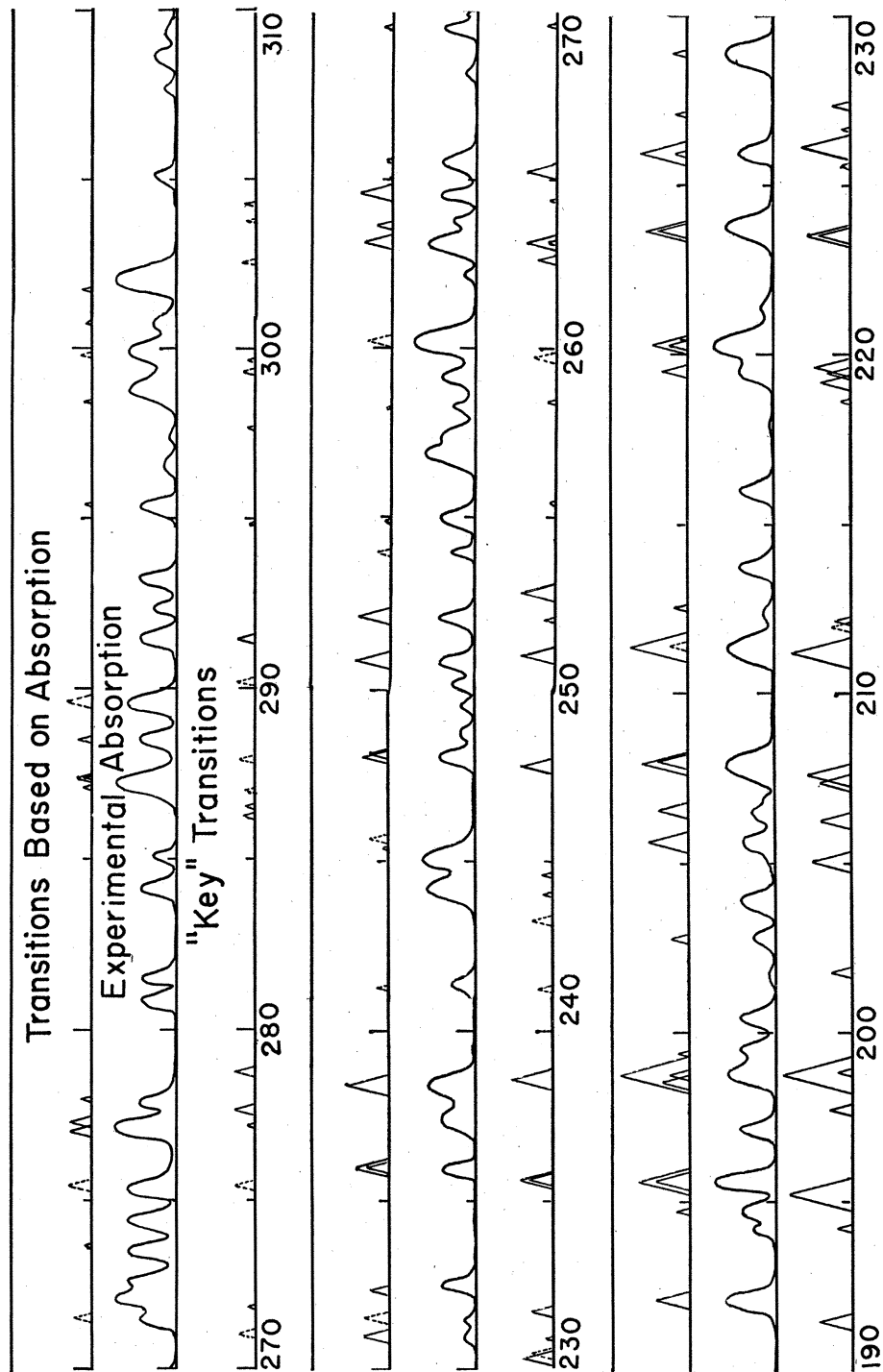
The method of analysis was essentially to identify the lines of the experimental data by means of a comparison with the "key" transitions, and then to construct a "true" or "adjusted" set of energy levels which were consistent with the data. Details of this process follow.

a. The key.—The key frequencies for allowed transitions were determined from the key energy levels together with the selection rules. Approximate intensities were calculated for as many transitions as possible. In Fig. 4 these key frequencies are plotted as similar isosceles triangles below the experimental data, the same frequency scale being used for both. The areas of the triangles have been chosen to be proportional to the intensities of the corresponding key transitions. (An unsuccessful attempt was made to plot theoretical intensities in terms of an experimentally determined absorption coefficient.)

b. The first assignment.—A study of the correlations between the experimental lines and the key transitions led to the observation that strong lines in the data occurred in general a few tenths of a wave number above intense lines in the key. Accordingly the first tentative assignment was made by the simple procedure of associating each key transition with the closest absorption line in the data which appeared to have a reasonably similar intensity. Further examinations of the two sets of lines were made to see if any other over-all assignment would be found upon shifting the key frequencies up or down by a few wave numbers together with proportional increase or decrease in line separations. No such alternative assignment gave nearly as satisfactory an account of the lines as did this first and most obvious one. It appeared reasonable, then, to assume that the preliminary choice of moments of inertia, together with the approximate corrections applied, had produced an energy level key which was rather close to the true level scheme sought.

c. Series regularities.—After making this first assignment a study of series regularities and combination relations brought about some adjustment, and occasionally a reassignment of transition frequencies, leading to the final values which are to be found plotted in the top lines of Fig. 4. More should be said about these aids in the analysis. It has been pointed out⁵ that there are analytic series regularities associated with the pairs of transitions which have a common value of $(j-k)$ when considered as symmetric rotator transitions. An example of one such series is given in Table VI, in which the regularity of the 2nd differences of the transitions based on

¹⁸ R. de L. Koenig, *Band Spectra and Molecular Structure* (Macmillan, 1930), p. 96.



(This figure is continued on opposite page.)

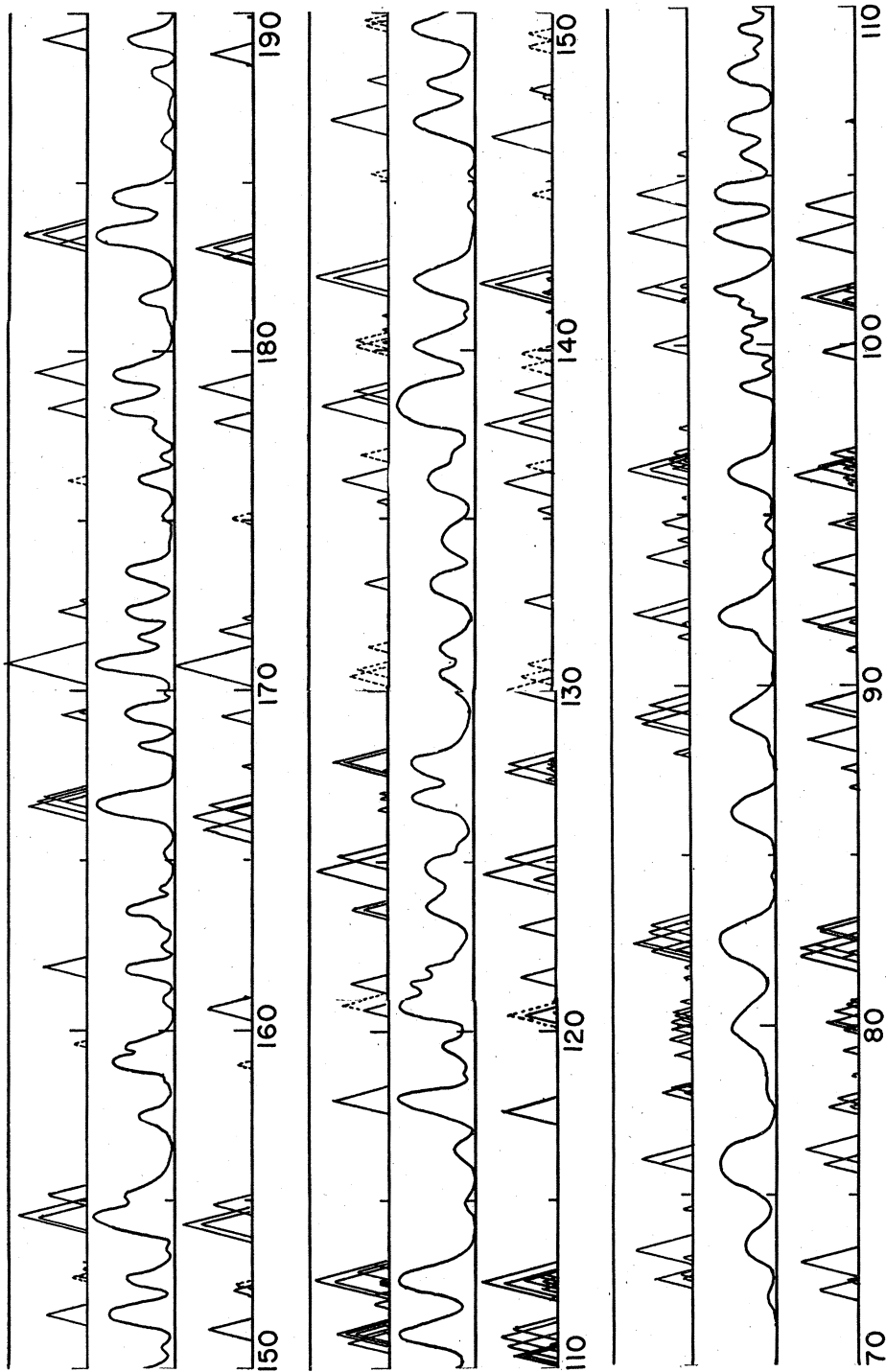


FIG. 4. Plot of D_2O frequencies in waves per centimeter. The bottom row of triangles is a graph of transitions between the key energy levels. The middle curve is a graph of the experimentally measured absorption spectrum of D_2O . The upper triangles represent the transition frequencies as assigned on the basis of the experimental data.

data is shown to compare favorably with those of the key transitions. Other groups of analytic series were found useful, though it will not be necessary to discuss the types in detail. In all, a dozen series were found which included five or more energy level transitions. A study of these series showed that the 2nd differences for the adjusted frequencies averaged 0.1 to 0.2 cm^{-1} greater than the corresponding 2nd differences in the key transition series.

Series with fewer than five terms were not useful for checking assignments. Also a number of series were composed of transition pairs of very low intensity and so did not aid much in the adjustment of frequencies. In some cases different series of the same type were nearly superposed upon each other, especially for the higher values of j . This superposition made assignments in these cases quite ambiguous. It also made it difficult if not impossible to correlate experimentally observed line intensities with calculated intensities of single or superposed transitions.

Extrapolation of the best series gave tentative assignments, consistent with the data, for transitions between some of the levels above $j=11$. The lowest series (low τ indices) could be extended up to $j=15$ with some degree of assurance. These extrapolated frequencies are plotted in Fig. 4 as broken-line triangles to differentiate them from those based more directly on comparisons with the computed key transitions.

d. Combination relations.—In order to further adjust values of transitions and to make the correct assignments two skeleton diagrams were drawn, one to show the allowed transitions between symmetric levels, and the other, between antisymmetric levels. (The numerical values of the energy levels themselves were not included until toward the end of the analysis.) This framework proved convenient in the process of visualizing and computing combination relations. Such relations were computed around as many closed circuits as possible. They were especially important in connecting the upper part of each diagram with the lower part, and in working out the consistency of the lower parts themselves, for series regularities gave little help in these regions.

Transitions of the vertical type (e.g., 6_6-6_4), and those so-called "inverted" transitions in which $\Delta\tau=4$ (e.g., 5_0-4_{-4}), were essential mem-

bers in each combination relation loop. Unfortunately these lines usually were of very small intensity. They were also in a great many cases almost exactly superposed both upon each other and upon other more intense transitions. This superposition (see Fig. 4) was so marked in the low frequency region that sometimes as many as eight transitions were assigned to an experimental absorption line which itself appeared single. Accordingly the frequencies of most of these vertical and inverse transitions could not be fixed more accurately than within a range of several tenths of a frequency unit. For convenience in the analysis these frequencies were so assigned within their allowed uncertainty range that combination relations gave zero sums around closed loops. Such circuit relations are, then, not to be considered more than rough checks on the consistency of the assignment. In Table III a suffix, *a*, distinguishes these arbitrarily adjusted frequencies from those whose values were sharply fixed by the experimental data. It should be mentioned that in the few cases where these weak transitions fell in isolated regions, their value was fixed by the experimental data, and such assignments could be used as criteria for judging the correctness of other lines.

e. Energy level assignment.—The transitions having been assigned in as satisfactory a manner as possible, the energy levels were obtained by assuming the correctness of the following key levels; 2_2 , 2_1 , 3_1 , and 3_0 . The rest of the energy levels were determined by means of transitions from these starting point levels. Eight low levels, 1_1 , 1_0 , 1_{-1} , 2_0 , 2_{-1} , 2_{-2} , 3_{-1} , 3_{-3} , were not reached by the assigned transitions. Key level values

TABLE VI. Highest series ($j-k=0$).

KEY SERIES				EXPERIMENTAL SERIES			
j	FREQ.	1ST DIFF.	2ND DIFF.	j	FREQ.	1ST DIFF.	2ND DIFF.
2	52.37			3	82.65		
3	82.62	30.25		4	112.59	29.94	
4	112.59	29.97	0.28	5	142.15	29.56	0.38
5	141.96	29.37	.60	6	170.81	28.77	.79
6	170.70	28.74	.63	7	198.78	27.97	.80
7	198.77	28.07	.67	8	225.94	27.16	.81
8	226.11	27.34	.63	9	252.09	26.15	1.01
9	252.80	26.69	.65	10	277.30	25.21	.94
10	278.77	25.97	.72	11	301.80	24.50	.71
11	304.23	25.46	.51				

TABLE VII. *Difference between experimental levels and key levels.*

$(j-k)$	$j=2$	3	4	5	6	7	8	9	10	11
0	0.00	0.03	0.04	0.21	0.32	0.33*	0.16	-0.55	-2.02	-4.45
1		.00	.23	.32	.55	.89	1.05*	.87	.17	-1.68
2			.38	.70	.97	1.25	1.60	1.75*	1.65	1.14
3				.60	.88	1.28	1.72	2.15	2.46*	2.45
4					1.00	1.39	1.93	2.38	2.70*	

were assigned to these also, no other method of assignment being possible. (2_{-2} and 3_{-3} were deducible each through a single weak inverse transition but key level values were adopted as giving the more reliable value.)

The levels of even τ value could be computed quite separately from those of odd τ value by means of the skeleton transition diagrams to which reference has been made. The consistency of the energy levels could, then, be checked at many points by the requirement that the even and odd τ indexed level pairs had to have identical values or small separation values given approximately by the key level separations.

These levels based on data are tabulated in Table IV. Column 1 shows the deviation of these experimental levels from the key levels. If the deviations are regrouped by series, as shown in Table VII for the five most important series, the amount of this deviation and the rate of increase of deviation with quantum number changes may be seen to show a reasonable regularity. It is also to be noted that in each series the deviations increase to a maximum then decrease, this maximum point (indicated by * in the body of Table VII) shifting to higher values of j as one goes from the highest toward the lower series.

IV. SUMMARY AND DISCUSSION

The experimental D_2O absorption frequencies together with their assignments as transitions between energy levels of the rotating D_2O molecule have been placed in Table III. Experimental and calculated intensities are also included in this tabulation. In Fig. 4 the top row is a plot of the experimentally assigned transition frequencies, the center row is an averaged plot of the experimental data, and the bottom row is a plot of the key frequencies which were computed quite independently of the experimental data here shown. A comparison of these three frequency diagrams gives a graphic picture of the

results of the analysis and shows how closely the key diagram fitted the actual data. From this analysis 184 rotational energy levels for the ground state of D_2O vapor have been evaluated. These have been recorded in Table IV.

210 absorption lines were observed experimentally. 192 key transitions were used in the analysis (this number included all transitions up through $j=11$ which had measurable intensities and which fell within the 75 cm^{-1} to 350 cm^{-1} range.) 111 distinct energy levels (single or fused doublets) resulted from the analysis. 24 levels above $j=11$ were tentatively assigned by means of 24 transitions consistent with the data. The maximum intensity of a fused pair of transitions was 170 units; for a single transition, 110 units. There were, in round numbers, 100 transitions with intensities less than 5 units, 50 with intensities between 5 and 20 units, 50 with intensities between 20 and 60 units, and 15 with intensities over 60 units.

The theoretical transition frequencies are well accounted for by the experimental absorption lines. The only transitions to which no satisfactory assignment could be made were (4_1-3_{-3}), ($8_{-1}-7_{-5}$), and ($11_{-2}-10_{-6}$) which were weak inverse transitions, and ($7_{-7}-6_{-5}$), a medium strong line which fell at the extreme long wavelength limit of the region covered by this experimental research, a region where the absorptions were very uncertain at best. This latter line was arbitrarily assigned to satisfy combination relations with lines, which were in more reliable regions from the experimental point of view, even if they were less intense. Incidentally this arbitrary assignment gave the desired amount of splitting of the two transitions making up a term in the lowest series, the other transition being independently assigned.

There were a large number of experimentally determined absorption lines for which no theoretical assignment could be made. Most of these were found in the high frequency region, where it was legitimate to assume that transitions between higher energy levels might be found to account for them if the analysis were to be extended to higher energy levels. There are, however, a number of lines in the low wave number range which could not be accounted for in this way, notably a medium strong line at 86.35

cm^{-1} , several medium lines lying between 98 cm^{-1} and 101.3 cm^{-1} , another group between 105 cm^{-1} and 110 cm^{-1} , as well as the following scattered strong and medium lines in the medium wave number range: 157.50 cm^{-1} , 159.10 cm^{-1} , 163.57 cm^{-1} , 173.58 cm^{-1} , and 184.69 cm^{-1} .

Neither were these lines to be explained as being due to H_2O impurities or to 2nd-order spectral impurities, as they did not coincide with the strongest H_2O lines or 2nd-order lines in the region. It was also quite improbable that they were spurious lines as they were found time and time again on different gratings and with different optical paths.

It is possible that the HDO impurities were not completely eliminated and thus were responsible for these absorptions. If so, it should be possible to eliminate them by a more complete drying out of the absorption cell. Another possibility is that certain of the allowed transitions whose intensities could not be calculated by means of the symmetric rotator matrix elements do, nevertheless, have measurable intensities and should be considered. Finally, there is the possibility

that the whole assignment of theoretical transitions has been incorrect. If this be true, then it means that the effective moments of inertia calculated in the analysis are greatly in error. The assignment would have to be completely reconsidered in order to account for these lines at all. As has been previously stated, several attempts were made during the analysis to find alternative assignments which would account for the experimental data, and none were found to be nearly as satisfactory as the one developed here.

Assuming the general correctness of the analysis however, the next problem is to develop rigorous methods of computing the rotational distortion of the asymmetric rotator so that the effective moments of inertia may be recomputed with precision from the energy levels obtained from this research. The dimensions of the molecule may then be well established.

One of the authors (N. F.) would like to acknowledge support from a Rackham Predoctoral Fellowship during 1937–38, the year in which the experimental part of this work was done.

Van der Waals Potential in Helium

H. MARGENAU

Yale University, New Haven, Connecticut

(Received September 22, 1939)

Part I is an investigation of the fundamental question concerning the additivity of first-order exchange and second-order van der Waals potentials. The method employed is a variational one which allows both first- and second-order exchange effects to be calculated simultaneously with the second-order attractive terms. It is shown that the assumption of additivity is entirely false for atomic hydrogen, but that it is almost legitimate for He. By extrapolation one might conclude it to be quite safe for heavier structures. Part II is a redetermination of the numerical values occurring in the attractive part of the potential, based on the use of oscillator strengths (f values) which are adjusted to give the best value for the atomic polarizability of He. It appears that the value of the dipole-dipole coefficient in the Slater-Kirkwood formula has been too high. The final result for the van der Waals potential (Eq. (20)) seems on the whole to be consistent with independent determinations of this quantity from empirical data.

NUMEROUS questions arising in the study of the behavior of helium at low temperatures require for their treatment a fairly accurate knowledge of the van der Waals potential between helium atoms.

Considerable attention has therefore been de-

voted¹⁻⁴ to attaining an empirical answer to the

¹ J. Lennard-Jones, Proc. Roy. Soc. **106**, 463 (1924).

² J. de Boer and A. Michels, Physica **5**, 945 (1938); **6**, 409 (1939).

³ J. O. Hirschfelder, R. B. Ewell and J. R. Roebuck, J. Chem. Phys. **6**, 205 (1938).

⁴ H. S. W. Massey and R. A. Buckingham, Proc. Roy. Soc. **168**, 378 (1938); **169**, 205 (1938).

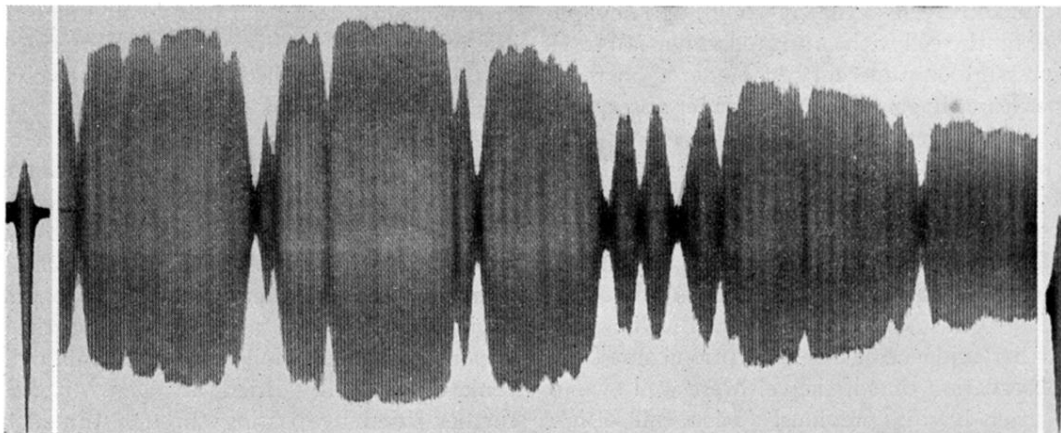


FIG. 1. H_2O vapor absorption in the region between $31\ \mu$ and $38\ \mu$, using an echelette grating with 600 lines per inch (total number of lines is 12,000), low temperature source, amplification factor of $\times 200$, path length equivalent to 60 cm of saturated H_2O vapor at room temperature, effective slit width of $0.3\ \text{cm}^{-1}$. The dispersion is rather good in this record, as the "true width" of a strong absorption line is roughly four times the effective slit width. (Lines $0.5\ \text{cm}^{-1}$ apart were separated but two strong doublets of $0.25\ \text{cm}^{-1}$ separation distance look single.) The resolution is excellent. Optical path consists of thorium-oxide-coated source, Aquadag-coated thermopile receivers, NaF *reststrahlen* plate, NaCl shutter, 1 mm Metastyrene and 4 mm paraffin wax as filters. This arrangement gave excellent purity as is evidenced by the almost complete absorption of the stronger lines.

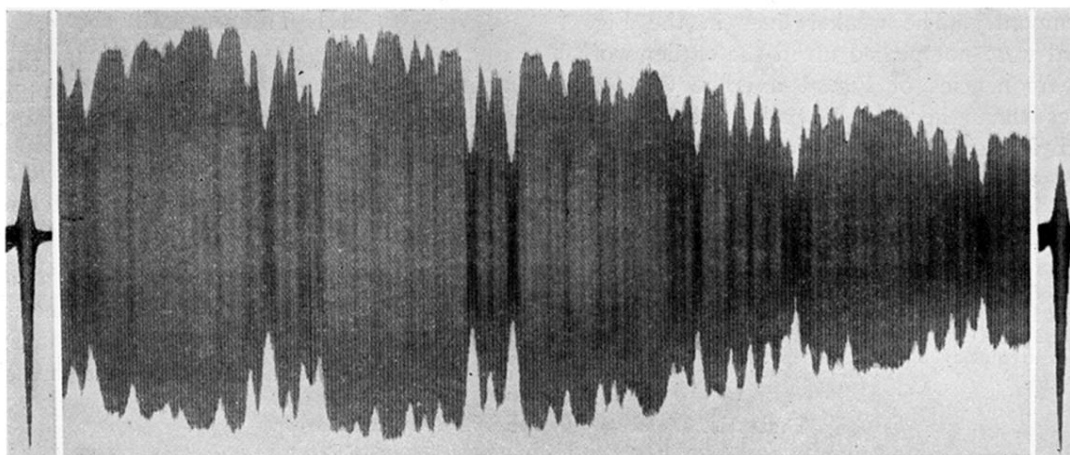


FIG. 2. D_2O vapor absorption in the same region and under identical conditions used for the H_2O record shown in Fig. 1. A comparison of the two records reveals that the D_2O lines are much weaker and much more numerous. The weakness is due partly to the fact that the D_2O transitions here recorded are between energy levels having higher quantum numbers than those for the H_2O record, and partly to the intrinsically greater strength of the H_2O absorptions. The greater number is a result of the greater mass of the molecular components of D_2O which cause a crowding together of all the energy levels.